We are IntechOpen, the world's leading publisher of Open Access books Built by scientists, for scientists

6,900
Open access books available

185,000
International authors and editors

200M
Downloads

154
Countries delivered to

Our authors are among the
TOP 1%
most cited scientists

12.2%
Contributors from top 500 universities

BOOK CITATION INDEX
CLARIVATE ANALYTICS
INDEXED

WEB OF SCIENCE™

Selection of our books indexed in the Book Citation Index
in Web of Science™ Core Collection (BKCI)

Interested in publishing with us?
Contact book.department@intechopen.com

FISH Probe Counting
in Circulating Tumor Cells

Sjoerd T. Ligthart, Joost F. Swennenhuis,
Jan Greve and Leon W.M.M. Terstappen
University of Twente
The Netherlands

1. Introduction

Presence of tumor cells in blood of patients with metastatic carcinomas has been associated with poor progression free and overall survival (Cohen et al., 2008; Cristofanilli et al., 2004; de Bono et al., 2008). Assessment of treatment targets on circulating tumor cells (CTC) before initiation of therapy may provide a means to guide therapy (Attard et al., 2009; de Bono et al., 2007; Hayes et al., 2002; Meng et al., 2006; Meng et al., 2004; Smirnov et al., 2005; Swennenhuis et al., 2009). Characterization of CTC can be performed by Fluorescence In Situ Hybridization (FISH) which has been used to prove that CTC are indeed malignant (Fehm et al., 2002; Swennenhuis, et al., 2009), and that gene amplifications, deletions and translocations related to certain therapies can be detected (Attard, et al., 2009; Meng, et al., 2006; Meng, et al., 2004).

CTC are extremely rare in most patients: 1-10/7.5 ml of blood (Allard et al., 2004), among about 50 million leukocytes and 50 billion erythrocytes within that volume. For accurate characterization of the CTC it is thus of utmost importance that no cell loss is incurred and the error in the interpretation of the results is kept to a minimum. The CellSearch® system is the only clinically validated system for counting CTC (Allard, et al., 2004; Kagan et al., 2002). It is based firstly on immunomagnetic enrichment of the blood sample using antibodies directed against the epithelial cell adhesion molecule (EpCAM). A second step consists of labeling the enriched sample with fluorescent dyes for the nucleus and cytokeratins 8, 18, and 19; CD45 labeling to recognize leukocytes. In a third step, fluorescence images are recorded of the enriched and labeled sample. CTC candidates are presented to a trained reviewer who distinguishes CTC from debris and leukocytes. Limitation of the CellSearch system is that only CTC expressing both EpCAM and CK8, 18 and or 19 will be detected.

Recently, we have developed a semi-automated method for FISH analysis of CTC after they have been identified by the CellSearch™ system. Interpretation of FISH results is however encumbered by apoptosis of CTC, which is observed frequently. In addition, counting of FISH dots can be tiring and subjective, and thus likely results in differences in intra-reviewer and inter-reviewer interpretation. Automation of counting of these FISH signals - termed FISH dots hereafter- could resolve these challenges. Other work has been done in the field of automated counting of FISH dots: on cell lines (Netten et al., 1997), blood from

healthy individuals (de Solorzano et al., 1998), cells from amniotic fluid (Lerner et al., 2001), and on tissue (Raimondo et al., 2005). An excellent overview of methods is available (Restif, 2006). However, to our knowledge, automated dot counting has never been applied in samples containing containing CTC. The nuclei and dots of these cells are extremely heterogeneous in shape and intensity, and therefore difficult to score, even by reviewers. Therefore, we investigated the error in counting FISH dots, and evaluated different methods to count the FISH dots by a computer algorithm.

2. Method

2.1 Patient samples

A prospective multicenter clinical trial that evaluated the utility of counting CTC for predicting response to therapy, progression-free survival, and overall survival in metastatic castration-resistant prostate cancer patients was conducted (de Bono, et al., 2008). A total of 65 clinical centers throughout the United States and Europe participated in this study after formal institutional review board approval. All patients were required to provide written informed consent. Blood was collected before starting a new treatment and at monthly intervals prior to the next cycle of therapy.

2.2 Sample preparation for CTC enumeration

Blood samples were drawn into 10 mL evacuated blood draw tubes, maintained at room temperature, and processed within 96 hours of collection. The CellSearch System (Veridex LLC, Raritan, NJ) consists of the CellTracks Autoprep®, CellTracks Magnest®, CellSearch Epithelial Cell Kit and the CellTracks Analyzer II®. The CellSearch™ Epithelial Cell Kit contains: -ferrofluids labeled with the epithelial cell adhesion molecule (EpCAM); -staining reagents 4',2-diamidino-2-phenylindole, (DAPI), CD45-Allophycocyan (CD45-APC), cytokeratin 8, 18 Phycoerythrin, cytokeratin 19 Phycoerythrin (CK-PE); buffers to enhance cell capture (Rao et al., 2005), cell permeabilization and cell fixation. The CellTracks Autoprep immuno-magnetically enriches cells expressing EpCAM from 7.5 ml of blood, fluorescently labels the enriched cells with DAPI, CD45-APC and CK-PE, and re-suspends the cells in the cartridge placed in the CellTracks Magnest. The design of the magnets guides the magnetically labeled cells to the analysis surface (Tibbe et al., 2002).

2.3 Data acquisition for CTC enumeration

The CellTracks Magnest containing the cartridge is placed on the CellTracks Analyzer II a semi-automated fluorescence-based microscopy system that acquires images using a 10X/0.45NA objective with filters for DAPI, FITC, PE, and APC to cover the complete surface area of the cartridge. The CellSearch software identifies objects staining with DAPI and PE in the same location and generates images for the DAPI, FITC, PE, and APC filters. A reviewer selects the CTC defined as nucleated DAPI+ cells larger than 4 μm, lacking CD45-APC and expressing CK-PE from the gallery of objects, which are tabulated by the computer. Figure 1 shows an overview of the image acquisition and identification of CTC. After a scan, the cartridges were stored at room temperature until the reviewer was finished reviewing the images. Accuracy, precision, linearity, and reproducibility of the CellSearch system have been described elsewhere (Allard, et al., 2004).
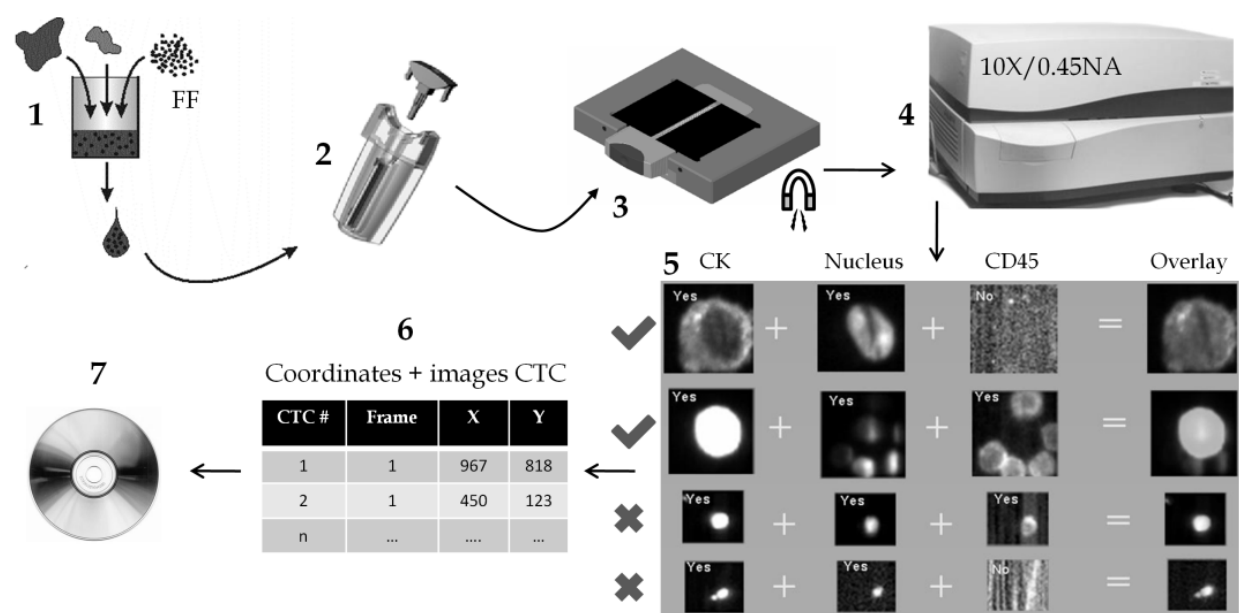
Fig. 1. Image acquisition in CellSearch. 1) Ferrofluid and staining reagents are added to the blood sample. 2) After immuno-magnetic enrichment and fluorescent labeling, the sample is inserted in a cartridge. 3) The cartridge is inserted into a Magnest to distribute the labeled cells over the analysis surface. 4) The cartridge is scanned at 10X in the CellTracks Analyzer. 5) CK+ DAPI+ objects are presented to the reviewer for CTC selection. 6) Coordinates of selected CTC are collected. 7) The coordinates and images from the scan are saved on a CD or DVD.

2.4 Samples used for FISH counting algorithm development

For algorithm development, images from cells of a patient in which no CTC were detected were used. Leukocytes which were non-specifically carried over during the CTC enrichment procedure were used as targets for this purpose, as in these cells almost no chromosomal aberrations are present and each cell should therefore contain two copies of each chromosome and gene region. The sample was labeled with a centromere specific FISH probe for chromosome 17 and a probe identifying the HER2 gene region. The centromere probe is larger than the HER2 probe, thus a difference in automated count could be expected. For the validation of the algorithm, CTC from 47 patients with hormone refractory metastatic prostate cancer labeled with probes identifying the centromeres of chromosome 1, 7, 8 and 17 were used (Swennenhuis, et al., 2009).

2.5 Sample preparation for FISH probes on CTC

Cartridges containing CTC were used for the FISH procedure. To preserve the location of the CTC for future interrogation the buffer inside the cartridge was carefully aspirated aspirated to avoid cell cell movement and replaced with methanol acetic acid. After fixation the cartridges are dried using a forced forced air flow flow and processed for FISH or stored at -20 °C for later use. FISH probes specific for the centromeric regions of chromosome 1, 7, 8, and 17 labeled with PlatinumBright-647, -550, -505, and -415, respectively, were used in this study (Kreatech, Amsterdam, The Netherlands). The probe mixture consisted of 50 µL

of hybridization buffer (50% Formamide / 1 x SSC / 10% Dextran Sulfate) containing FISH probes against 1, 7, 8, and 17 at 2 ng/μL each. The cartridges were placed on a 80°C hotplate for 2 min, with the glass facing towards the hotplate, and hybridized at 42°C for 16 h. After hybridization the cartridge was washed with PBS containing DAPI (use abbreviation instead of whole word) as a nuclear counter stain.

2.6 Data acquisition for FISH probe detection in CTC

After hybridizing the FISH probes, the samples were scanned on a modified CellTracks Analyzer II. This analyzer is equipped with a 40X/0.63NA objective, to improve the resolution and light collection of the fluorescent FISH dots, and filter cubes to detect DAPI, Platinum*Bright*-647, -550, -505, and 415. The locations and images of the CTC identified in the initial 10X scan -described in 2.3- were loaded from a CD. A software program was written to move to the locations of interest and record Z-stacks to capture signals at a range of depths of the objects of interest (Swennenhuis, et al., 2009). The DAPI signals are used to correlate the 40X with the 10X scan, thereby verifying if the CTC location is correct. This was necessary, as the cells could shift up to ~200 μm due to the FISH protocol. The image acquisition procedure for the FISH probe detection is shown in figure 2.
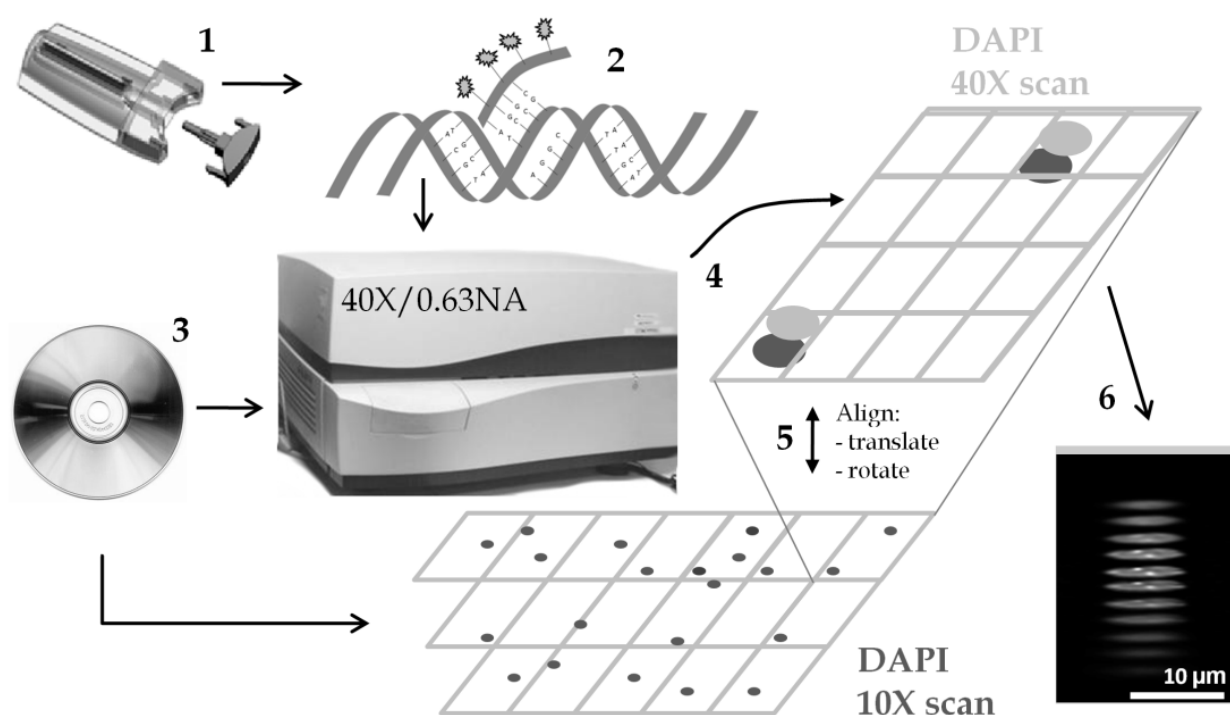

Fig. 2. Procedure for FISH probe imaging. 1) The cartridge is re-opened to carefully aspirate buffer and fixate the cells. 2) FISH reagents are added and the sample is hybridized for 16h. 3) Coordinates and images from previously assigned CTC are loaded from a CD. 4) The modified CellTracks records DAPI images at 40X at the designated coordinates and surroundings. 5) Cross correlation is performed between the DAPI images from the 40X and 10X scan to verify the correct location of the CTC. 6) After the right location is found, the FISH z-stacks are recorded.

2.7 Algorithm for counting FISH signals in leukocytes and CTC

Maximum intensity profiles were created of all the Z-stacks to speed up the counting process for human reviewing. The algorithm to identify the nucleus and count the FISH probes within this nucleus consists of five general steps:

1. enhancement and segmentation of the outline of the nucleus;
2. enhancement and segmentation of potential FISH objects;
3. exclusion of objects that are too noisy;
4. measurement of intensity and morphological features of the potential objects;
5. exclusion of objects that do not meet inclusion criteria.

Nuclei were located in the DAPI image, which was enhanced using a zero-crossing filter in combination with a gradient magnitude filter (Verbeek & Vanvliet, 1994). Edges were enhanced using a morphological gradient magnitude filter. The image of this filter was multiplied by an image filtered by a laplace-plus-dgg filter. This filter created a combination of second order derivatives in x and y, and combined it with an image of the second derivative in the direction of the maximum gradient. The combined image of the two filters is thresholded using a fixed threshold. On the outline of objects larger than 2000 pixels a distance transform was applied: every outline pixel value is replaced by its closest distance to the edge of the outline. This procedure was then followed by a watershed transform, to verify if the outline consisted of multiple maxima and were thus two or more closely spaced objects. Figure 3 shows how a distance transform improves the watershed transform in case of saturated DAPI signals. The nucleus that was at least 250 pixels in size and located closest to the middle of the image was selected as the final outline: only objects inside this outline are considered for FISH dot counting.
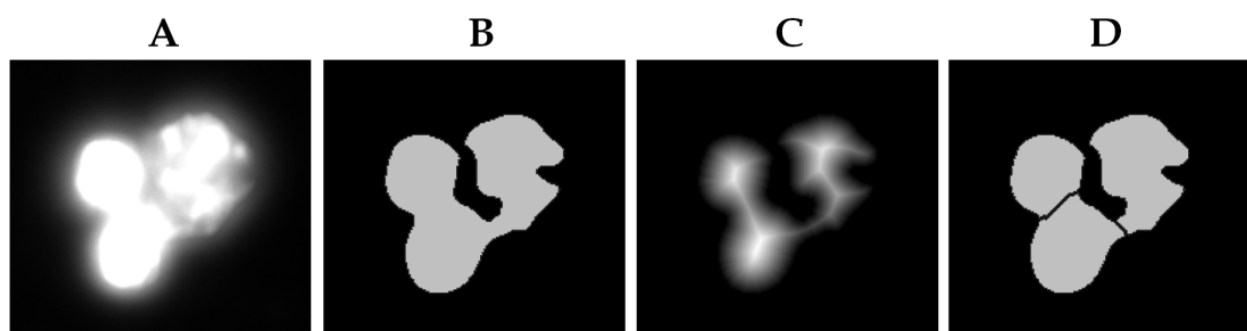

Fig. 3. Example of a distance transform aiding the watershed transform. Panel A shows the original DAPI image containing three nuclei which is thresholded to give the outline at panel B. This outline is difficult to watershed due to saturation in the original image. The distance transform shown in panel C creates a new input for the watershed transform, which successfully separates the nuclei as is shown in panel D.

In a next step, dot-like structures were enhanced. Usually this is performed by employing a tophat filter (Netten, et al., 1997). We used a method termed multiscale product (Vermolen et al., 2008) because it appeared better suited to deal with the heterogeneity of the shapes of the FISH probes. This filter increases the intensity of objects in a range of radii, using a multiplication of Gaussian kernels with different σ (ranging from 1.5 to 3.0 pixels):

$$G_{product} = (G - G_0) \cdot (G_0 - G_1) \cdot (G_1 - G_2) \tag{1}$$

with the 2D Gaussian kernel defined as

$$G(\sigma_i) = \frac{1}{2\pi\sigma_i^2} e^{-\frac{x^2+y^2}{2\sigma_i^2}} \tag{2}$$

Using a range of Gaussian kernel sizes improves robustness to variations in size of the objects of interest, compared to using a single kernel size as is done in the tophat transform method. After applying the multiscale product, objects were thresholded using the triangle threshold (Zack et al., 1977) which was multiplied by a factor of 0.1 to include all relevant dot-like structures, bright or dim. This thresholding method uses the intensity histogram of the image and is especially suited for images with few object pixels. After thresholding, a final verification was performed to exclude objects that are too noisy. The dome finding method of Restif was applied to the coordinates of the maximum of each object (Restif, 2006). This method checks nearest downhill neighbors in three level sets -up to three pixels around the maximum- and excludes objects that have more than one extra local maximum in this region. Figure 4 shows the method by which nearest downhill neighbors are checked.
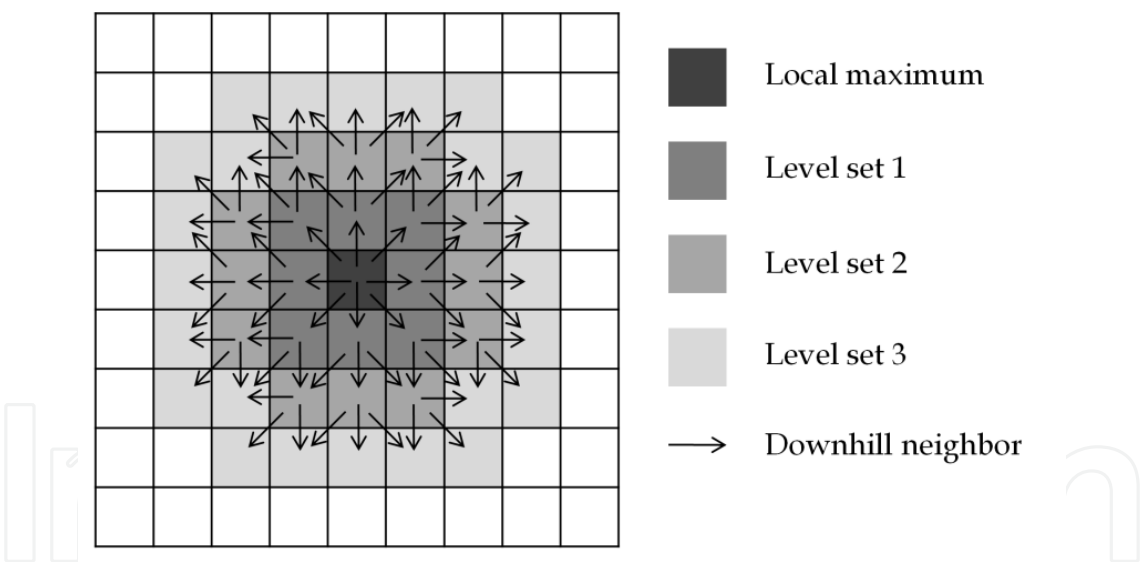

Fig. 4. Scheme for checking downhill neighbors. By checking objects in this way only dome shape objects are included. (adapted from (Restif, 2006))

Restif et al. determined that if one extra local maximum is allowed, at least 75% of the downhill neighbors should have a lower intensity. We allow one extra local maximum to include very closely spaced FISH dots. In this way, noisy objects are excluded, whether or not this noise is originating from a high or low intensity background. Finally, measurements were performed on these objects: size, maximum intensity, mean intensity, total intensity, relative intensity, roundness, and perimeter were saved for every object. Relative intensity was defined as the total intensity of the object related to the total intensity of the brightest

object within the same nucleus. Using these measurements, different exclusion criteria were tested. Combinations of measurements were tested on the leukocyte training set to exclude debris and keep the true FISH dots. Figure 5 gives a schematic overview of the procedure.
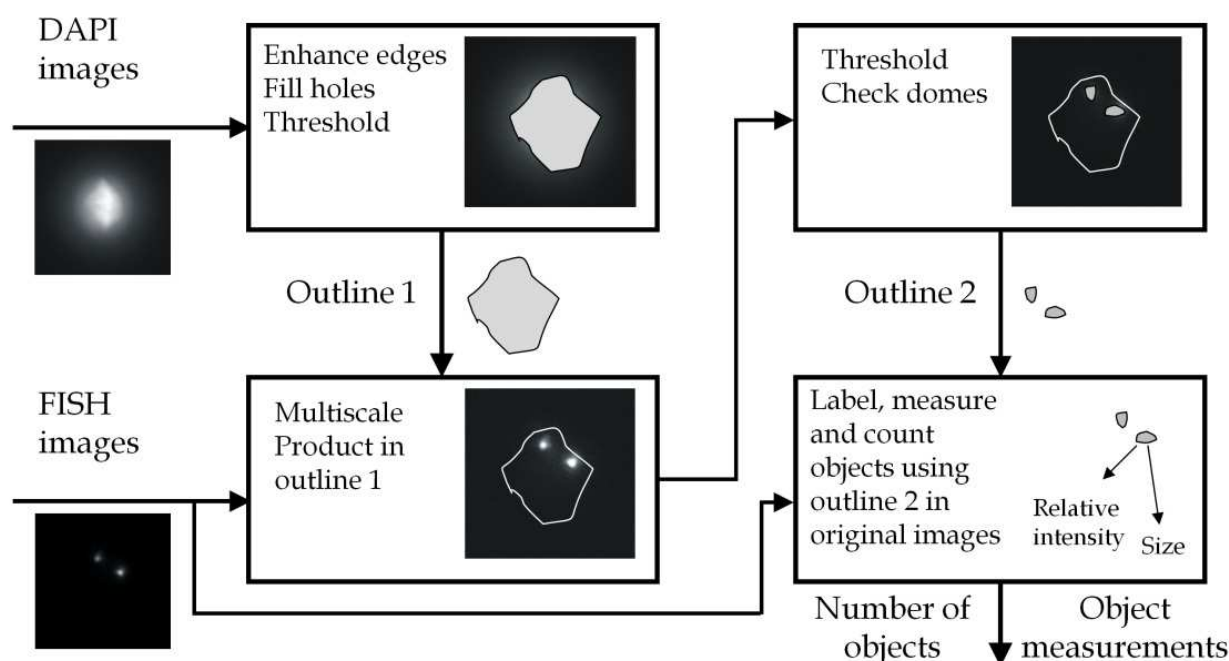

Fig. 5. Schematic representation of the counting process. DAPI images are loaded and their outline is determined. Within this outline, a multiscale product is applied. Objects within outline 1 are thresholded and checked for dome-like structures. Finally, the objects are counted and measured.

2.8 Expert reviewing of samples

Next to the algorithm, five expert reviewers counted FISH probe signals in the leukocytes, using a macro written in the program ImageJ (Collins, 2007). They reviewed the set two times: the first time they were asked to review all images, the second time they could skip images that were unclear in their view. In this way it could be measured how sure reviewers were. All CTC samples were also reviewed by the five expert reviewers.

3. Results

492 leukocytes and 500 CTC were imaged by the modified CellTracks Analyzer II. Figure 6 shows an example of a FISH Z-stack from a leukocyte in top and slice view, from which a maximum profile was created. The profiles were processed by the algorithm, requiring ~2 minutes for each sample and counted by human reviewers, requiring ~2 hours for each sample. Figure 7 shows the different steps of the algorithm: segmentation of the nucleus, enhancement of dot-like structures and the final outline of nucleus and the dots.
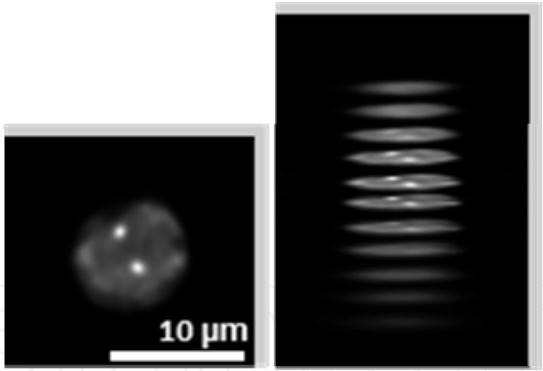
Fig. 6. Example of a recorded Z-stack of FISH probes in a leukocyte in top-view, panel A, and in slice-view, panel B. Distance between the slices is 1 µm
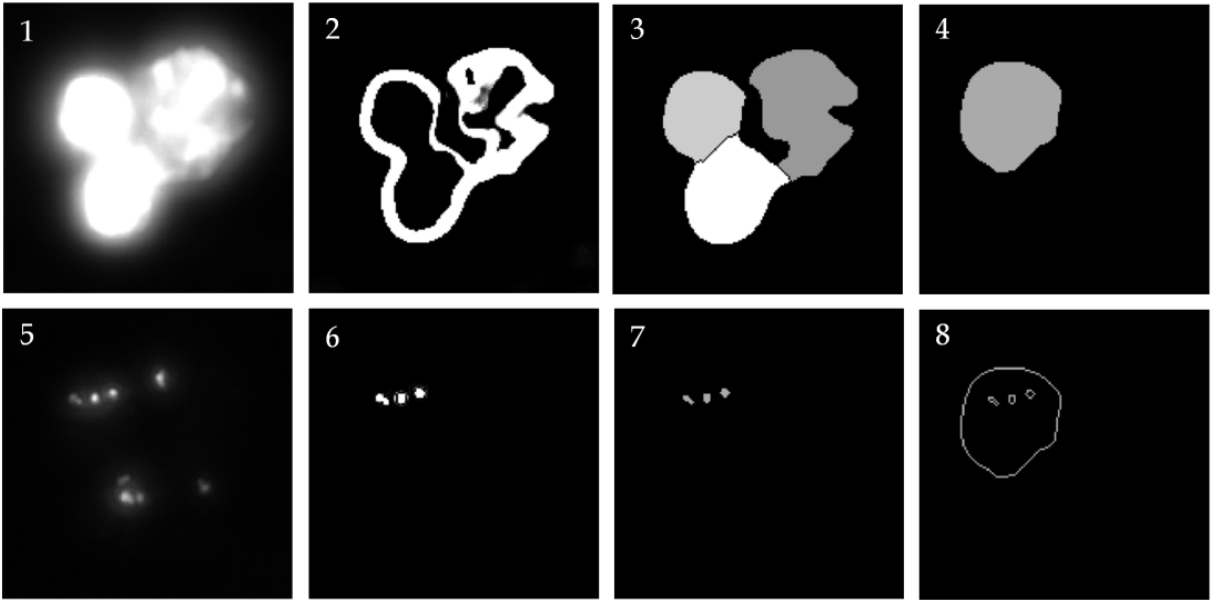

Fig. 7. Example of the image processing steps on a recorded DAPI and FISH image. 1) original DAPI image; 2) edge enhanced DAPI image; 3) outline after thresholding and watershed; 4) final DAPI outline; 5) original FISH image; 6) FISH image after multiscale product; 7) outline FISH image; 8) final outlines of DAPI and FISH.

3.1 Counting of the leukocyte training sample

After comparison of the manual and automated counts in the training sample, it became apparent that only the measurements "size" and "relative intensity" had a positive impact on the counting efficiency of the algorithm. After objects were measured and counted in the HER2 channel the objects, with a relative intensity lower than 30% of the brightest dot, within that nucleus were excluded. For the centromere 17 channel this threshold was optimal at 25%. Objects smaller than 5 pixels were also excluded. Automatic counting of chromosomes in leukocytes resulted in an accuracy of 97.8% of the HER2 dots and 97.5% of the centromere 17 dots. Accurate here means "equal to the manual count of the subset of images were all reviewers agreed upon" (n=409 for HER2 and n=347 for centromere 17). The

mean inter-reviewer agreement was 92.6%±2.3% and 91.7%±1.7% and the mean intra-reviewer agreement was 96.5%±2.7% and 97.0%±1.8% for the HER2 and centromere 17 probes, respectively. Table 1 gives an overview of the counting efficiencies after review of HER2 and centromere 17 of the whole data set and the data set containing only the images with objects that could be easily identified by the reviewer, compared with the count generated by the algorithm. In figure 8 the distribution of the count of the PC and five reviewers are shown. The count of the reviewers is represented by the mean and the standard deviation for each chromosome count.

HER2	Rev 1	Rev 2	Rev 3	Rev 4	Rev 5	PC
Rev 1	96.2%±1.7%	91.3%±2.5%	93.9%±2.1%	93.5%±2.2%	95.5%±1.9%	90.3%±2.6%
Rev 2	91.3%±2.5%	92.5%±2.3%	89.9%±2.7%	89.3%±2.7%	90.9%±2.6%	85.0%±3.2%
Rev 3	93.9%±2.2%	91.0%±2.6%	95.7%±1.8%	92.7%±2.3%	96.0%±1.8%	90.5%±2.6%
Rev 4	98.7%±1.2%	97.7%±1.6%	97.9%±1.5%	99.2%±1.0%	92.9%±2.3%	87.6%±2.9%
Rev 5	97.3%±1.5%	93.0%±2.3%	96.2%±1.8%	99.2%±1.0%	98.9%±1.0%	92.1%±2.4%
PC	90.5%±2.6%	87.4%±2.9%	89.8%±2.7%	96.9%±1.8%	92.6%±2.4%	100.0%-0.4%
Cent17						
Rev 1	96.4%±1.7%	92.9%±2.3%	92.7%±2.3%	93.7%±2.2%	90.5%±2.6%	87.6%±2.9%
Rev 2	92.3%±2.4%	94.9%±2.0%	93.9%±2.1%	90.7%±2.6%	92.3%±2.4%	88.1%±2.9%
Rev 3	95.0%±2.0%	94.5%±2.1%	96.0%±1.8%	90.3%±2.6%	91.7%±2.5%	85.4%±3.1%
Rev 4	96.1%±1.9%	98.3%±1.3%	97.0%±1.7%	99.0%±1.0%	88.5%±2.8%	89.1%±2.8%
Rev 5	96.0%±1.9%	96.0%±1.9%	98.1%±1.4%	96.4%±1.9%	98.6%±1.2%	88.5%±2.8%
PC	87.4%±2.9%	91.5%±2.5%	88.4%±2.9%	95.4%±2.1%	91.7%±2.7%	100.0%-0.4%

Table 1. Agreement between expert reviewers and the PC algorithm when reviewing leukocytes. In the upper right part of the table (white), the agreement of the first review is shown in which the reviewer had to review the full dataset (n=492). Second, in the lower left part of the table (dark grey) the agreement of the second review is shown, in which the reviewers only reviewed the cells they were certain of (the "obvious" dataset). Last, the intra-reviewer variation is given on the diagonal of the table (light grey).
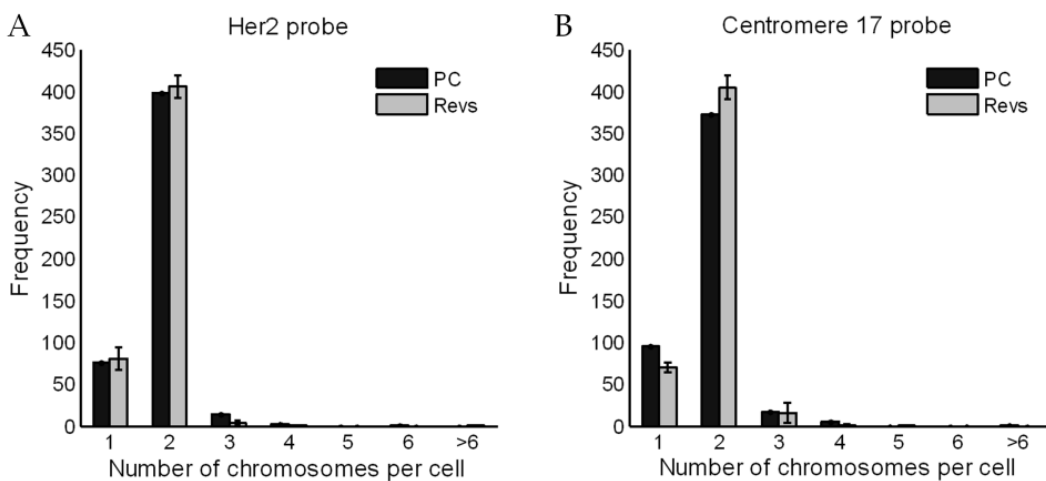

Fig. 8. Number of leukocytes for the HER2 gene probe (panel A) and the centromere of chromosome 17 probe (panel B) as counted by the PC and the five reviewers (n=492).
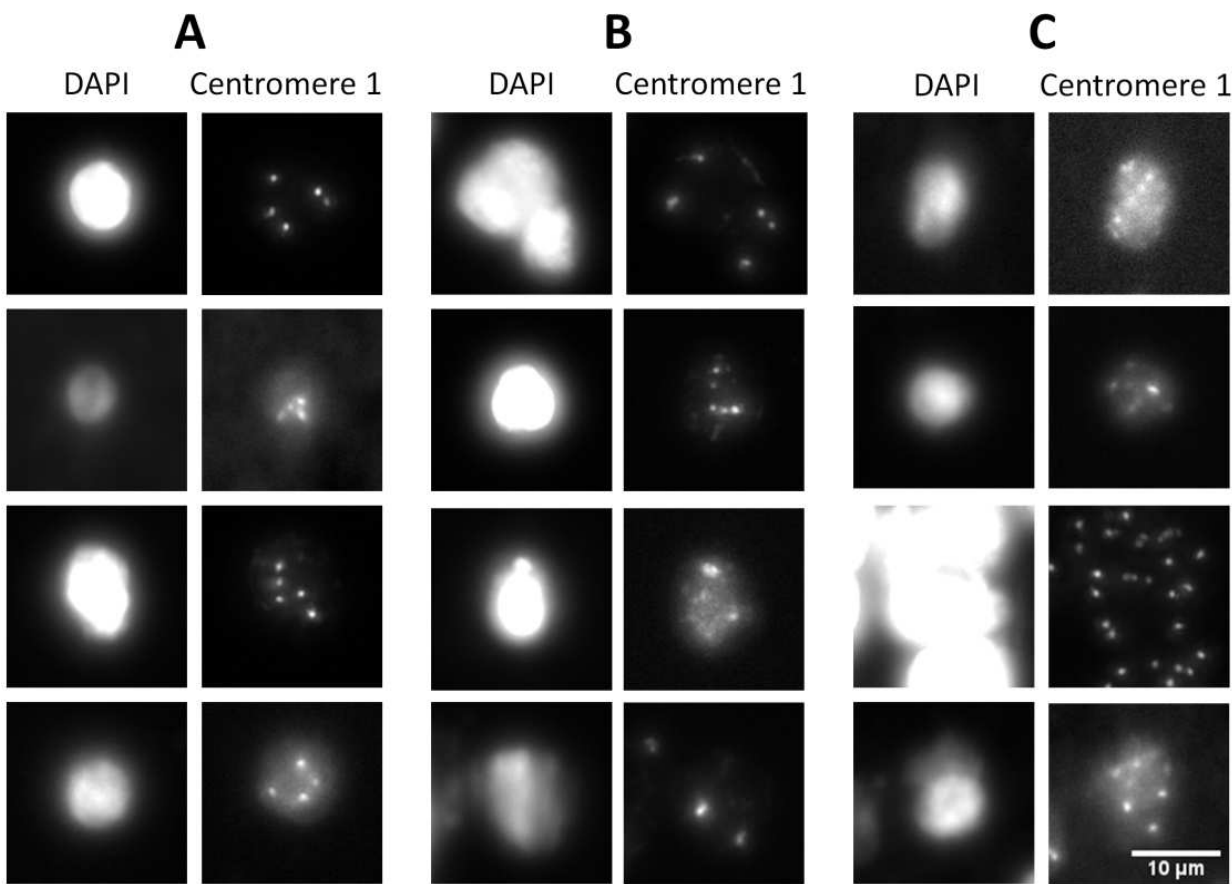
Fig. 9. Example of FISH images. Panel A shows cases were all reviewers and the PC agreed. Panel B shows examples were all the human reviewers agreed, but the PC disagreed on the number of FISH dots. Panel C shows examples with the largest discrepancy among reviewers.

3.2 Counting of a sample containing CTC

After processing a sample containing CTC it became clear that the threshold for relative intensity was strongly related to the quality of the FISH probe used, and thus probe dependent. Slight adjustment of the relative intensity criteria to a range from 14%-20% was necessary to ensure reasonable counting by the algorithm. This value was correlated with the average of the maximum intensity of all the objects in a channel: if this average was high, then the relative intensity should be set lower. Figure 9 shows three categories of examples from the data set: panel A shows examples were all the reviewers and the PC agreed; panel B shows examples were all reviewers agreed, *but the PC did not;* finally, panel C shows examples where there was a large discrepancy between all reviewers and the PC.

Agreement of the PC with the subset of cells on which all reviewers agreed was 76.1% (n=238), 83.9% (n=280), 86.6% (n=209), and 85.3% (n=251) for probes from centromere 1, 7, 8, and 17 respectively. Mean inter-reviewer agreement was 70.9%, 75.3%, 66.8%, and 72.3% for these four channels. Figure 10 show the agreement between all reviewers in detail and the histogram of the count.
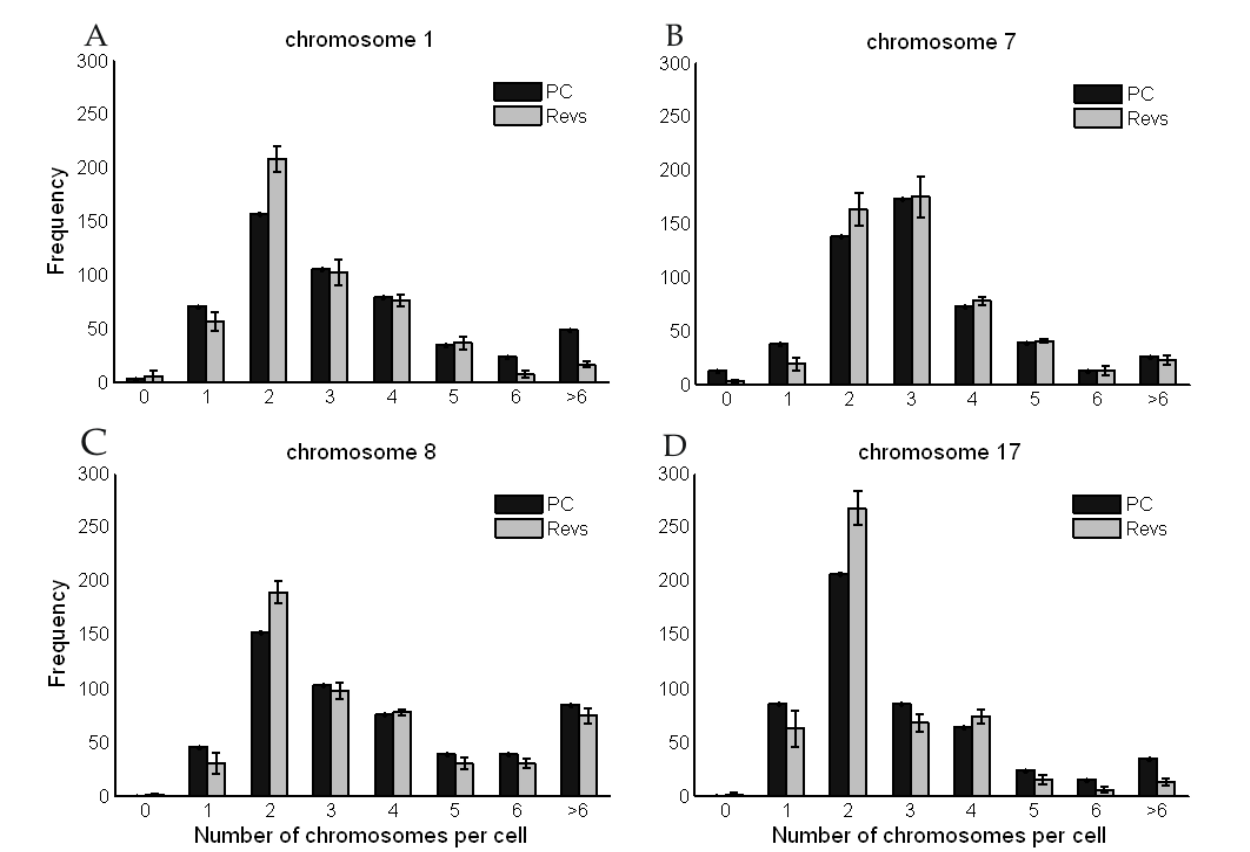
Fig. 10. Number of CTC containing 0-6 or >6 dots for the centromere of chromosomes 1,7,8, and 17 probe (panel A-D) as counted by the PC and the five reviewers (n=500). The reviewer count is given as the mean of the frequency of each number and its standard deviation.

4. Conclusion

4.1 Automated counting is necessary and feasible

We have shown that reliable automated counting of FISH probes on EpCAM+DAPI+CK+CD45- cells is both necessary and feasible. Comparing expert reviews revealed that intra-reviewer variation -the same expert reviewing a data set twice- could be as high as 3.5% of the cells. Inter-reviewer variation was higher: 7.5%; these numbers were both acquired for the "easy" leukocyte samples with low copy numbers. Variation between reviewers while reviewing CTC samples could be as high as 33.2% (centromere chromosome 8), showing that the number of signals in a nucleus is of great influence on counting accuracy, as is the knowledge of the reviewer that he or she is dealing with CTC or leukocytes. Furthermore, reviewing 500 FISH nuclei in four channels takes several hours, while the computer only needs a few minutes.

From the results it becomes clear that review of chromosome 1 and 8 was the most difficult, for both PC and reviewer. These probes had on average a factor two lower intensities than the probes from chromosomes 7 and 17. Thus, the inter-reviewer agreement was lower as well as the agreement with the PC. The dome finding part of the algorithm revealed the same: it removed objects that were too noisy in 17% and 13% of the nuclei in the channel from chromosome 1 and 8 respectively, and only in 8% of the nuclei from channels of chromosome 7 and 17. Signal to noise ratios were clearly lower in channels were the agreement was lower.

4.2 Sources of error for human and PC

Agreement between PC and reviewer was good when control samples were reviewed, and reasonable when CTC were reviewed. The difference between the two data sets could be attributed to a few main sources of error:

1. Nuclei were well separated in the leukocyte sample, the CTC samples contained more clusters. While these clusters are usually easily resolved by eye, the algorithm had more difficulty in this task. Figure 9, panel B shows an example in row 1: two closely spaced nuclei with almost saturated intensity. In this case the signals of the nuclei are close to saturation and although a distance transform and watershed transform was applied, they were still segmented as one. The PC thus over-counted in this example.

2. Because the DAPI signal from the nuclei can vary greatly between samples, some signals fall just outside the segmented outline of the nucleus as determined by the algorithm. This is the case when the signal from the nucleus is relatively dim, as is shown in figure 9, panel B, row 4, where the reviewers counted two probes and the PC counted only one. This challenge could be resolved by dilating the outline nuclei more than is done now. However, closely spaced nuclei will be resolved worse in this case. The heterogeneity of the shape and size of the nucleus is largely due to presence of ferrofluid in combination with the fixation step in the FISH procedure. The ferrofluid particles were added to keep the cells tightly located to the imaging surface. However, due to the influence of these magnetic particles and the tendency of some cells to adhere to surfaces, the DNA spreads over the surface. Ferrofluid particles that line up under influence of the magnetic field force these cells to spread even further. Thus in the DAPI images even small islands of DNA were visible, that clearly were part of a bigger nucleus, making it more difficult for the algorithm to measure a perfect outline of the nucleus and include all the DNA in the dot counting. Figure 11 shows an example of this effect.
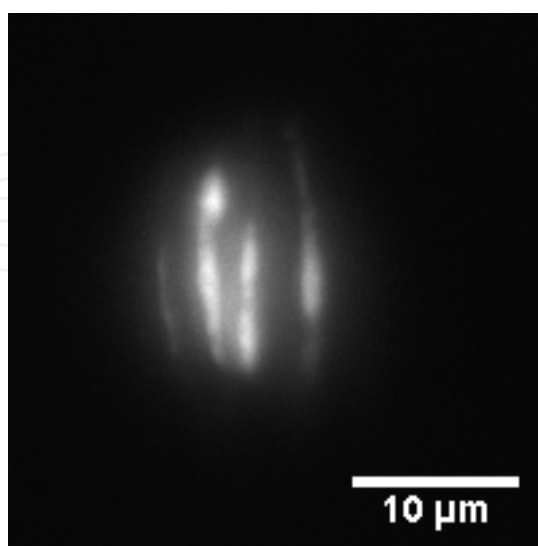

Fig. 11. Example of a nucleus spread due to fixation of the cell. Note the vertical lines that were created by ferrofluid aggregates that follow the local magnetic field. This type of nucleus is especially difficult to segment correctly.

3. The CTC sample had a larger variety in signal quality. Although the segmentation algorithm is dynamic on the histogram, it is still difficult for the PC to distinguish between what a reviewer calls a "true signal" and debris. For example, when a reviewer sees two signals -a bright and a relatively dim one-, he or she will usually count two. However, when five bright signals and one dim signal are seen, the dim object is more often neglected. Figure 9 panel B rows 2 and 3 show examples of difference in counting because of relative intensity. In row 2, the reviewers counted five and the pc four, while in row three, the reviewers counted two and the PC three probes. The PC counts 100% reproducible, but does not take into account these human considerations. For this analysis, it is thus very difficult to get an absolute "golden truth".

4. It still is hard for the PC to distinguish between a split probe (one chromosome that had two signals) and two closely spaced chromosomes. It is however not known how often a reviewer misclassifies such an object. A reviewer can structurally ignore or assign the split spots. The PC cannot and counts these items according to the algorithm. The number of cells that have these split spots may vary between samples and also within samples (e.g. between lymphocyte and CTC). The PC might not be able to distinguish between these, but if this factor appears to be of influence to the result, the PC could use the measurements of the probes -i.e. relative intensity coupled to size of closely spaced probes- to estimate the probability of these splits in the cells. Leukocytes could be used as an internal control for measuring the frequency of these splits and for estimating a relevant "size/relative intensity" threshold.

The above error sources may seem a big challenge, but are not of importance for the clinical relevant observations, which is the presence or absence of aneuploidy to ascertain the cancerous origin of the cells and the presence of amplification or deletions of specific genes that may be used to guide certain therapies. CTC are very heterogeneous: within one patient a wide variety of chromosomal aberrations could be spotted. So whether or not a certain cell has five or six copies is of lesser importance than the fact that this number is greater than two. When comparing counts that are greater than two or not, the reviewer and PC concur in 87%, 93%, 94%, and 94% of the cells for centromere 1, 7, 8, and 17 respectively for the data set in which all reviewers agree. This demonstrates that in about 90% of the cases, the PC and reviewer will draw the same conclusion about the ploidy status of the cells identified as tumor cells.

Figure 9 panel C shows examples in which the reviewers greatly disagreed. Two examples of varying signal intensities (rows 1 and 2) and two examples of difficulty of locating the true outline of the nucleus (row 3 en 4) are given. It could be argued that the example of row 1 isn't suitable for reviewing at all because the background staining is too high. For reviewers, there is no real quantitative criterion whether or not to reject a certain object based on its intensity distribution. However, the PC has such a criterion: it can easily check if a maximum of an object is surrounded by more than two other local maxima. If this is the case, then an object should be excluded. We perform this verification by means of the dome finding function. In this way, the PC performs more reliable than the human reviewers.

4.3 Future research

In the future, the algorithm may be optimized further by using clinical data. When coupling for instance response to a therapy of a patient to the aberration of the genes in the CTC the

treatment is targeting, a better golden truth may be found. Furthermore, quality of FISH could still be improved. Split probes are still a big challenge for the PC, but also for establishing a good count by reviewers. Consequently a quality score could be set by the algorithm by measuring intensity variations, for instance in carried-over leukocytes. This score could be used as an internal control in each patient sample to adjust exclusion criteria and to reject cells that are not suitable for interpretation. Finally, removal of ferrofluid could greatly improve the segmentation of the nucleus. Aggregation of ferrofluid particles disturbs the natural shape of the nucleus and blocks a fraction of the fluorescence light. Implementation of physical filters to enrich CTC by size would not require any ferrofluid and could be an improvement in the next generation tumor cell capturing devices.
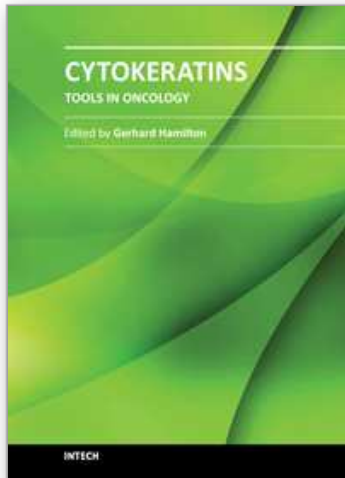
5. Acknowledgments

6. References

Allard, W. J.; Matera, J.; Miller, M. C.; Repollet, M.; Connelly, M. C.; Rao, C.; Tibbe, A. G. J.; Uhr, J. W. & Terstappen, L. (2004). Tumor cells circulate in the peripheral blood of all major carcinomas but not in healthy subjects or patients with nonmalignant diseases, *Clinical Cancer Research,* Vol.10, No.20, (Oct 2004), pp. 6897-6904, ISSN 1078-0432

Attard, G.; Swermenhuis, J. F.; Olmos, D.; Reid, A. H. M.; Vickers, E.; A'Hern, R.; Levink, R.; Coumans, F.; Moreira, J.; Riisnaes, R.; Oommen, N. B.; Hawche, G.; Jameson, C.; Thompson, E.; Sipkema, R.; Carden, C. P.; Parker, C.; Dearnaley, D.; Kaye, S. B.; Cooper, C. S.; Molina, A.; Cox, M. E.; Terstappen, L. & de Bono, J. S. (2009). Characterization of ERG, AR and PTEN Gene Status in Circulating Tumor Cells from Patients with Castration-Resistant Prostate Cancer, *Cancer Research,* Vol.69, No.7, (Apr 2009), pp. 2912-2918, ISSN 0008-5472

Cohen, S. J.; Punt, C. J. A.; Iannotti, N.; Saidman, B. H.; Sabbath, K. D.; Gabrail, N. Y.; Picus, J.; Morse, M.; Mitchell, E.; Miller, M. C.; Doyle, G. V.; Tissing, H.; Terstappen, L. & Meropol, N. J. (2008). Relationship of circulating tumor cells to tumor response, progression-free survival, and overall survival in patients with metastatic colorectal cancer, *Journal of Clinical Oncology,* Vol.26, No.19, 2008), pp. 3213-3221, ISSN 0732-183X

Collins, T. J. (2007). ImageJ for microscopy, *Biotechniques,* Vol.43, No.1, (Jul 2007), pp. 25-+, ISSN 0736-6205

Cristofanilli, M.; Budd, G. T.; Ellis, M. J.; Stopeck, A.; Matera, J.; Miller, M. C.; Reuben, J. M.; Doyle, G. V.; Allard, W. J.; Terstappen, L. & Hayes, D. F. (2004). Circulating tumor cells, disease progression, and survival in metastatic breast cancer, *New England Journal of Medicine,* Vol.351, No.8, (Aug 2004), pp. 781-791, ISSN 0028-4793

de Bono, J. S.; Attard, G.; Adjei, A.; Pollak, M. N.; Fong, P. C.; Haluska, P.; Roberts, L.; Melvin, C.; Repollet, M.; Chianese, D.; Connely, M.; Terstappen, L. & Gualberto, A. (2007). Potential applications for circulating tumor cells expressing the insulin-like growth factor-I receptor, *Clinical Cancer Research,* Vol.13, No.12, (Jun 2007), pp. 3611-3616, ISSN 1078-0432

de Bono, J. S.; Scher, H. I.; Montgomery, R. B.; Parker, C.; Miller, M. C.; Tissing, H.; Doyle, G. V.; Terstappen, L.; Pienta, K. J. & Raghavan, D. (2008). Circulating Tumor Cells Predict Survival Benefit from Treatment in Metastatic Castration-Resistant Prostate Cancer, *Clinical Cancer Research,* Vol.14, No.19, (Oct 2008), pp. 6302-6309, ISSN 1078-0432

de Solorzano, C. O.; Santos, A.; Vallcorba, I.; Garcia-Sagredo, J. M. & del Pozo, F. (1998). Automated FISH spot counting in interphase nuclei: Statistical validation and data correction, *Cytometry,* Vol.31, No.2, (Feb 1 1998), pp. 93-99, ISSN

Fehm, T.; Sagalowsky, A.; Clifford, E.; Beitsch, P.; Saboorian, H.; Euhus, D.; Meng, S. D.; Morrison, L.; Tucker, T.; Lane, N.; Ghadimi, B. M.; Heselmeyer-Haddad, K.; Ried, T.; Rao, C. & Uhr, J. (2002). Cytogenetic evidence that circulating epithelial cells in patients with carcinoma are malignant, *Clinical Cancer Research,* Vol.8, No.7, (Jul 2002), pp. 2073-2084, ISSN 1078-0432

Hayes, D. F.; Walker, T. M.; Singh, B.; Vitetta, E. S.; Uhr, J. W.; Gross, S.; Rao, C.; Doyle, G. V. & Terstappen, L. (2002). Monitoring expression of HER-2 on circulating epithelial cells in patients with advanced breast cancer, *International Journal of Oncology,* Vol.21, No.5, (Nov 2002), pp. 1111-1117, ISSN 1019-6439

Kagan, M.; Howard, D.; Bendele, T.; Mayes, J.; Silvia, J.; Repollet, M.; Doyle, J.; Allard, J.; Tu, N.; Bui, T.; Russell, T.; Rao, C.; Hermann, M.; Rutner, H. & Terstappen, L. (2002). A sample preparation and analysis system for identification of circulating tumor cells, *Journal of Clinical Ligand Assay,* Vol.25, No.1, (Spr 2002), pp. 104-110, ISSN 1081-1672

Lerner, B.; Clocksin, W. F.; Dhanjal, S.; Hulten, M. A. & Bishop, C. M. (2001). Automatic signal classification in fluorescence in situ hybridization images, *Cytometry,* Vol.43, No.2, (Feb 1 2001), pp. 87-93, ISSN 0196-4763

Meng, S.; Tripathy, D.; Shete, S.; Ashfaq, R.; Saboorian, H.; Haley, B.; Frenkel, E.; Euhus, D.; Leitch, M.; Osborne, C.; Clifford, E.; Perkins, S.; Beitsch, P.; Khan, A.; Morrison, L.; Herlyn, D.; Terstappen, L.; Lane, N.; Wang, J. & Uhr, J. (2006). uPAR and HER-2 gene status in individual breast cancer cells from blood and tissues, *Proceedings Of The National Academy Of Sciences Of The United States Of America,* Vol.103, No.46, (Nov 2006), pp. 17361-17365, ISSN 0027-8424

Meng, S. D.; Tripathy, D.; Shete, S.; Ashfaq, R.; Haley, B.; Perkins, S.; Beitsch, P.; Khan, A.; Euhus, D.; Osborne, C.; Frenkel, E.; Hoover, S.; Leitch, M.; Clifford, E.; Vitetta, E.; Morrison, L.; Herlyn, D.; Terstappen, L.; Fleming, T.; Fehm, T.; Tucker, T.; Lane, N.; Wang, J. Q. & Uhr, J. (2004). HER-2 gene amplification can be acquired as breast cancer progresses, *Proceedings Of The National Academy Of Sciences Of The United States Of America,* Vol.101, No.25, (Jun 2004), pp. 9393-9398, ISSN 0027-8424

Netten, H.; Young, I. T.; vanVliet, L. J.; Tanke, H. J.; Vroljik, H. & Sloos, W. C. R. (1997). FISH and chips: Automation of fluorescent dot counting in interphase cell nuclei, *Cytometry,* Vol.28, No.1, (May 1 1997), pp. 1-10, ISSN 0196-4763

Raimondo, F.; Gavrielides, M. A.; Karayannopoulou, G.; Lyroudia, K.; Pitas, I. & Kostopoulos, I. (2005). Automated evaluation of Her-2/neu status in breast tissue from fluorescent in situ hybridization images, *Ieee Transactions On Image Processing,* Vol.14, No.9, (Sep 2005), pp. 1288-1299, ISSN 1057-7149

Rao, C. G.; Chianese, D.; Doyle, G. V.; Miller, M. C.; Russell, T.; Sanders, R. A. & Terstappen, L. (2005). Expression of epithelial cell adhesion molecule in carcinoma cells present

in blood and primary and metastatic tumors, *International Journal of Oncology,* Vol.27, No.1, (Jul 2005), pp. 49-57, ISSN 1019-6439

Smirnov, D. A.; Zweitzig, D. R.; Foulk, B. W.; Miller, M. C.; Doyle, G. V.; Pienta, K. J.; Meropol, N. J.; Weiner, L. M.; Cohen, S. J.; Moreno, J. G.; Connelly, M. C.; Terstappen, L. & O'Hara, S. M. (2005). Global gene expression profiling of circulating tumor cells, *Cancer Research,* Vol.65, No.12, (Jun 2005), pp. 4993-4997, ISSN 0008-5472

Swennenhuis, J. F.; Tibbe, A. G.; Levink, R.; Sipkema, R. C. & Terstappen, L. W. (2009). Characterization of circulating tumor cells by fluorescence in situ hybridization, *Cytometry Part A,* Vol.75, No.6, (Jun 2009), pp. 520-7, ISSN 1552-4930 (Electronic)

Tibbe, A. G. J.; de Grooth, B. G.; Greve, J.; Dolan, G. J.; Rao, C. & Terstappen, L. (2002). Magnetic field design for selecting and aligning immunomagnetic labeled cells, *Cytometry,* Vol.47, No.3, (Mar 2002), pp. 163-172, ISSN 0196-4763

Verbeek, P. W. & Vanvliet, L. J. (1994). On the location error of curved edges in low-pass filtered 2-D and 3-D images, *Ieee Transactions on Pattern Analysis and Machine Intelligence,* Vol.16, No.7, (Jul 1994), pp. 726-733, ISSN 0162-8828

Vermolen, B. J.; Garini, Y.; Young, I. T.; Dirks, R. W. & Raz, V. (2008). Segmentation and analysis of the three-dimensional redistribution of nuclear components in human mesenchymal stem cells, *Cytometry Part A,* Vol.73A, No.9, (Sep 2008), pp. 816-824, ISSN 1552-4922

Zack, G. W.; Rogers, W. E. & Latt, S. A. (1977). Automatic-Measurement Of Sister Chromatid Exchange Frequency, *Journal of Histochemistry & Cytochemistry,* Vol.25, No.7, 1977), pp. 741-753, ISSN 0022-1554

Cytokeratins - Tools in Oncology

Edited by Dr. Gerhard Hamilton

The first chapters of the volume "Cytokeratins - Tools in Oncology" discuss multiple functions of cytokeratins in organization of the intermediary filaments in normal intestine and liver as well as microfold L cells and the usability of cytokeratins 7, 8 and 20 in tumor diagnosis in detail. Epithelial to mesenchymal transition as a mechanism important in pathogenesis is touched in another chapter, followed by several articles dealing with the role of cytokeratins for detection of disseminated tumor cells and as response markers during chemotherapy. This book is therefore destined to all cancer researchers and therapists who want to understand the diagnostic application of cytokeratins in histology and, especially, the use of anti-cytokeratin antibodies to identify viable residual tumor cells accounting for a higher risk of tumor recurrence or cancer cells responding to chemotherapy, respectively.

How to reference

In order to correctly reference this scholarly work, feel free to copy and paste the following:

Sjoerd T. Ligthart, Joost F. Swennenhuis,Jan Greve and Leon W.M.M. Terstappen (2012). FISH Probe Counting in Circulating Tumor Cells, Cytokeratins - Tools in Oncology, Dr. Gerhard Hamilton (Ed.), ISBN: 978-953-51-0047-8, InTech, Available from: http://www.intechopen.com/books/cytokeratins-tools-in-oncology/fish-probe-counting-in-circulating-tumor-cells

INTECH
open science | open minds